Optimization of Efficiency in the Glyoxalase Pathway†

Donald J. Creighton,* Molly Migliorini, Tayebeh Pourmotabbed, and Mrinal K. Guha
Laboratory for Chemical Dynamics, Department of Chemistry, University of Maryland Baltimore County, Catonsville, Maryland 21228

Received September 29, 1987; Revised Manuscript Received May 4, 1988

ABSTRACT: A quantitative kinetic model for the glutathione-dependent conversion of methylglyoxal to D-lactate in mammalian erythrocytes has been formulated, on the basis of the measured or calculated rate and equilibrium constants associated with (a) the hydration of methylglyoxal, (b) the specific base catalyzed formation of glutathione–(*R*,*S*)-methylglyoxal thiohemiacetals, (c) the glyoxalase I catalyzed conversion of the diastereotopic thiohemiacetals to (*S*)-D-lactoylglutathione, and (d) the glyoxalase II catalyzed hydrolysis of (*S*)-D-lactoylglutathione to form D-lactate and glutathione. The model exhibits the following properties under conditions where substrate concentrations are small in comparison to the K_m values for the glyoxalase enzymes: The overall rate of conversion of methylglyoxal to D-lactate is primarily limited by the rate of formation of the diastereotopic thiohemiacetals. The hydration of methylglyoxal is kinetically unimportant, since the apparent rate constant for hydration is ($\sim$500–10^3)-fold smaller than that for formation of the thiohemiacetals. The rate of conversion of methylglyoxal to (*S*)-D-lactoylglutathione is near optimal, on the basis that the apparent rate constant for the glyoxalase I reaction ($k_{cat}E_t/K_m \simeq$ 4–20 s^{-1} for pig, rat, and human erythrocytes) is roughly equal to the apparent rate constant for decomposition of the thiohemiacetals to form glutathione and methylglyoxal [k(obsd) = 11 s^{-1}, pH 7]. The capacity of glyoxalase I to use both diastereotopic thiohemiacetals, versus only one of the diastereomers, as substrates represents a 3- to 6-fold advantage in the steady-state rate of conversion of the diastereomers to (*S*)-D-lactoylglutathione. The steady-state concentration of free glutathione in the cell is maintained at near-optimal levels for the amount of glyoxalase I in the cell, on the basis that the apparent rate constant for the glyoxalase II reaction ($k_{cat}E_t/K_m \simeq$ 3 s^{-1} for rat erythrocytes) is roughly equal to that for the glyoxalase I reaction.

The ubiquitous glyoxalase enzyme system, composed of glyoxalases I (Glx I,[1] EC 4.4.1.5) and II (Glx II, EC 3.1.2.6), catalyzes the GSH-dependent conversion of methylglyoxal to D-lactate (eq 1). The glyoxalase pathway has been suggested

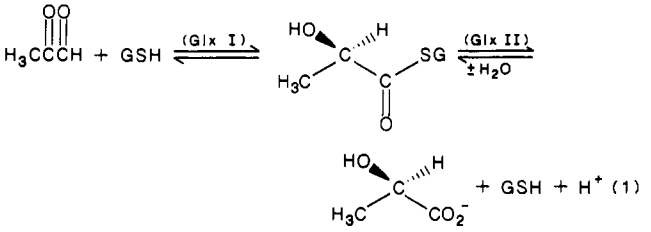

to play a role in regulating cell growth in normal and neoplastic tissues by altering the intracellular concentrations of growth-inhibitory α-ketoaldehydes (Együd & Szent-Györgyi, 1966). However, the absence of any clear evidence for allosteric control of the glyoxalase enzymes suggests that the principle function of the pathway is simply to chemically remove cytotoxic methylglyoxal from cells as D-lactate. In mammalian cells, methylglyoxal may arise from several possible sources including the uncatalyzed (Needham & Lehmann, 1937; Riddle & Lorenz, 1968; Richard, 1984) and the triosephosphate isomerase catalyzed (Browne et al., 1976; Cambell et al., 1979) dismutation of intracellular trioses and triose phosphates. In support of a detoxification role for the glyoxalase pathway, a mutant strain of the yeast *Saccharomyces cerevisiae*, defective in glyoxalase I, is eventually killed by exposure to glycerol and excretes methylglyoxal into the growth medium (Penninckx et al., 1983).

The aim of the present work is to assess how well the glyoxalase enzyme system is adapted to the efficient removal of methylglyoxal from cells. This assessment encompasses the fact that the glyoxalase system potentially operates on an equilibrium mixture of substrate forms composed of methylglyoxal, the mono- and dihydrates of methylglyoxal, and two diastereotopic thiohemiacetals (eq 2). A unified picture

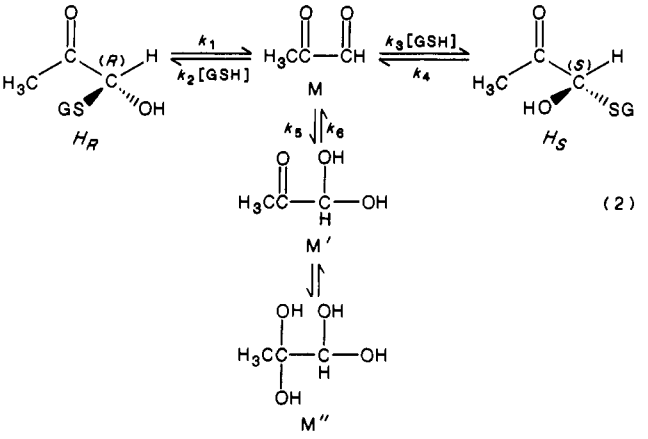

of the probable kinetic factors controlling the conversion of methylglyoxal to D-lactate in cells emerges from a comparison of the experimentally determined or calculated magnitudes of the microscopic rate constants of eq 2 and the kinetic properties and approximate amounts of glyoxalases I and II in mammalian erythrocytes, used here as a model cell. In several respects, the glyoxalase system is well adapted to its

† This work was supported by a grant from the National Institutes of Health (GM 31840).

[1] Abbreviations: Glx I, glyoxalase I; Glx II, glyoxalase II; GSH, glutathione; M, methylglyoxal; MTG, methyl thioglycolate; H_R and H_S, diastereotopic thiohemiacetals formed from GSH and methylglyoxal in which the chirality at the thiohemiacetal carbon is *R* and *S*, respectively; H_{R+S}, $H_R + H_S$; NMR, nuclear magnetic resonance; DSS, sodium 4,4-dimethyl-4-silapentanesulfonate.

0006-2960/88/0427-7376$01.50/0

presumed detoxification role in the cell.

Experimental Procedures

Materials. GSH from Sigma (type IV) was used without further purification and assayed to be ~95% pure by weight, on the basis of a sulfhydryl group assay using 4-pyridine disulfide (Aldrich) (Grassetti & Murray, 1967). Phenylglyoxal (Aldrich) was twice recrystallized from hot water. Methylglyoxal was synthesized by acid-catalyzed hydrolysis of the corresponding dimethyl acetal and purified by steam distillation (Pourmotabbed & Creighton, 1986). Methyl thioglycolate (Aldrich) and 2-mercaptoethanol (Sigma) were both purified by vacuum distillation under nitrogen shortly before use.

Equilibrium Constants. The apparent dissociation constants for the thiohemiacetals formed from phenylglyoxal and GSH, 2-mercaptoethanol, or methyl thioglycolate are defined as follows:

$$K_{diss} \simeq [\text{mercaptan}][\text{phenylglyoxal}]_t/[\text{thiohemiacetal}] \quad (3)$$

where $[\text{phenylglyoxal}]_t$ equals the sum of the concentrations of the free aldehyde and hydrated forms. In aqueous solution, phenylglyoxal is >99% as the aldehydrol (Hine & Koser, 1971). The magnitudes of the dissociation constants were determined by sequentially adding known amounts of mercaptan into a cuvette containing 0.1 mM phenylglyoxal and recording the increase in optical density at 280 nm due to the appearance of the thiohemiacetal. The dissociation constants were obtained from the ratios of the slopes and intercepts of reciprocal plots of the observed increase in optical density (ΔOD_{280}) versus the analytical concentrations of mercaptan present (0.2–1.0 mM). Glutathione does not absorb significantly at 280 nm.

Rate Constants. Rapid kinetic measurements were taken on an Aminco-Bowman stopped-flow spectrophotometer in which temperature control was maintained with a Haake variable-temperature bath. Stock solutions of the thiohemiacetals were prepared immediately before being used in the stopped-flow spectrophotometer. First-order rate constants were obtained by manually taking data from a photograph of the oscilloscope trace, followed by nonlinear regression analysis of the data over 3–4 half-lives. Constant ionic strength was maintained with KCl.

The rate constants for hydrolysis of (*S*)-D-lactoylglutathione in buffered solutions were determined in duplicate from the first-order decrease in optical density at 240 nm, due to loss of the thioester bond, in the temperature-controlled cuvette carriage of a Gilford 2400-2 spectrophotometer.

Determination of Glyoxalase I Activity in Porcine Erythrocytes. Fresh pig blood (~800 mL) was obtained from a local slaughterhouse, stabilized with sodium citrate, and stored at 4 °C overnight. The erythrocytes were collected by centrifugation (6000g, 20 min) and twice washed with 500-mL portions of ice-cold, aqueous 0.9% NaCl (w/v). The packed cells (450 mL) were suspended in 600 mL of ice-cold water and stirred for 1 h at 4 °C. After centrifugation, the supernatant was assayed for activity on the basis of the initial rate of increase in OD_{240}, due to the formation of (*S*)-D-lactoylglutathione, in the presence of GSH (3 mM) and methylglyoxal (3 mM) under the buffer conditions given in Table III. Under these assay conditions, the enzyme is essentially saturated with the substrate thiohemiacetal formed from GSH and methylglyoxal. Activities were calculated per milliliter of packed cells. Glyoxalase I activity was demonstrated to be completely released from erythrocytes after 1 h under the above conditions of cell lysis.

Results

The formulation of a quantitative kinetic model for the conversion of methylglyoxal to D-lactate in erythrocytes critically depends upon the relative magnitudes of the decomposition rate constants for H_R and H_S (k_1 and k_4) and the relative efficiencies with which H_R and H_S are used by glyoxalase I. That both H_R and H_S are used directly as substrates by glyoxalase I from yeast and from porcine erythrocytes was previously demonstrated by the ability of high concentrations of glyoxalase I to convert both $[^3H]H_R$ and $[^3H]H_S$ (formed from phenylglyoxal and [^{3}H]GSH) to ^{3}H-labeled product before exchange with unlabeled GSH (Griffis et al., 1983). The results were consistent with the enzyme using the two thiohemiacetals with roughly equal k_{cat}/K_m efficiencies. Moreover, the average rate constant for dissociation of H_R and H_S [$(k_1 + k_4)/2$] was estimated to be in the range 10–40 s^{-1} (pH 7), on the basis of the fractional trapping of radioactivity into product versus enzyme concentration.

Kinetic Measurements. A stopped-flow method has now been devised that gives a more accurate assessment of the magnitudes of k_1 and k_4, as well as their pH and buffer ion dependencies. Dissociation rate constants for thiohemiacetals due to simple aldehydes and mercaptans can be directly calculated from the observed rate constants for approach to equilibrium and the measured equilibrium constants (Barnett & Jencks, 1969). However, for the more complex system of eq 2, a method was needed that would more directly measure dissociation rate constants and, hence, would be more sensitive to possible differences in the relative magnitudes of k_1 and k_4. Attempts were made to measure these rate constants using kinetic systems in which the glutathione liberated from the dissociation of the thiohemiacetal was irreversibly trapped with 4-pyridine disulfide or Ellman's reagent. However, these trapping reactions were not efficient enough to make dissociation clearly rate determining. The final method of choice involved the use of excess methyl thioglycolate to trap the phenylglyoxal liberated from the dissociation of the thiohemiacetal. The progress of the reaction was then followed on the basis of the greater absorptivity of the thiohemiacetal formed from phenylglyoxal and glutathione versus the absorptivity of the thiohemiacetal formed from methyl thioglycolate [$\Delta\epsilon$(350 nm) = 91 M^{-1} cm^{-1}] (Figure 1).

This method was first used to determine the dissociation rate constant for the simple thiohemiacetal formed from phenylglyoxal and 2-mercaptoethanol. The difference absorption spectrum of the thiohemiacetals due to 2-mercaptoethanol and to methyl thioglycolate is similar to that shown in Figure 1. Observed rate constants [k(obsd)] were obtained either by introducing methyl thioglycolate into solutions of 2-mercaptoethanol thiohemiacetal and following the first-order decrease in optical density at 350 nm or by introducing 2-mercaptoethanol into solutions of methyl thioglycolate thiohemiacetal and following the first-order increase in optical density at 350 nm. In principle, both methods are kinetically equivalent since k(obsd) reflects the approach to an equilibrium

$$\text{H} \underset{k_\beta[\text{S}]}{\overset{k_\alpha}{\rightleftharpoons}} \text{P} \underset{k_\delta}{\overset{k_\gamma[\text{MTG}]}{\rightleftharpoons}} \text{H}' \quad (4)$$

where H = thiohemiacetal formed from 2-mercaptoethanol, S = 2-mercaptoethanol, P = phenylglyoxal, MTG = methyl thioglycolate, and H′ = thiohemiacetal formed from methyl thioglycolate. Under conditions where [S] and [MTG] ≫ [H] and [H′], the apparent rate constant in the forward direction (k_f) is related to the microscopic rate constants by k_f =

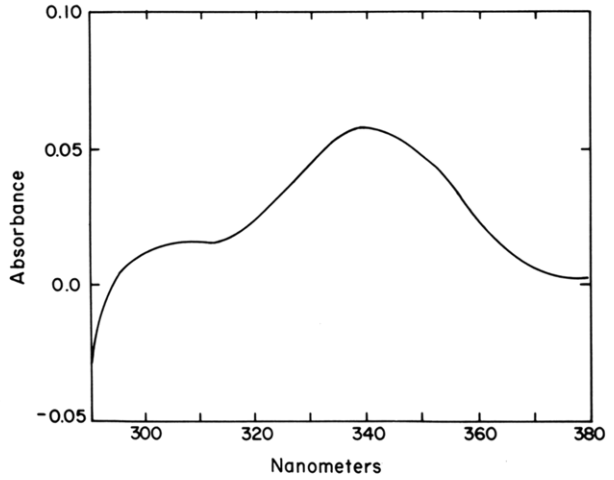

FIGURE 1: Ultraviolet difference absorption spectrum of the thiohemiacetal formed from glutathione and phenylglyoxal versus that formed from methyl thioglycolate and phenylglyoxal. The solutions in the sample and reference cuvettes were made up to contain equal concentrations of the two different thiohemiacetals, on the basis of the experimentally determined dissociation constants (Table I). Sample cuvette: [thiohemiacetal] = 0.52 mM, [glutathione] = 19.1 mM, [phenylglyoxal] = 0.05 mM. References cuvette: [thiohemiacetal] = 0.52 mM, [methylthioglycolate] = 12.1 mM, [phenylglyoxal] = 0.05 mM. Conditions: phosphate buffer (0.3 M, pH 6.20), $\Gamma/2$ = 1.5 M, 25 °C.

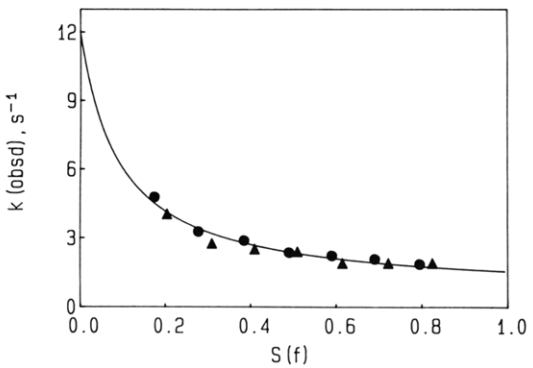

FIGURE 2: Variation of k(obsd) versus S_f for the thiohemiacetals formed from 2-mercaptoethanol and methyl thioglycolate with phenylglyoxal (eq 4). In the first series of stopped-flow experiments (●), k(obsd) values were obtained from the first-order decrease in optical density at 350 nm of the observation chamber, into which one syringe delivered 2-mercaptoethanol thiohemiacetal (2.95 mM) plus successively decreasing concentrations of free mercaptoethanol (77–17 mM) and the other syringe delivered successively increasing concentrations of methyl thioglycolate (20–80 mM). In each experiment, [methyl thioglycolate] + [2-mercaptoethanol] = 97 mM. In the second series of experiments (▲), k(obsd) values were obtained from the first-order increase in optical density at 350 nm of the observation chamber, into which one syringe delivered methyl thioglycolate thiohemiacetal [2.98 mM] plus successively decreasing concentrations of free methyl thioglycolate (77–17 mM) and the second syringe delivered successively increasing concentrations of 2-mercaptoethanol (20–80 mM). In each experiment, [methyl thioglycolate] + [2-mercaptoethanol] = 97 mM. The error in the values of k(obsd) is in the range 2–5%, on the basis of random error in the data points over 3–4 half-lives. The solid line through the data of the figure was calculated from eq 5 in which R is experimentally fixed at 1.52, k_α = 1.54 ● 0.06 s^{-1}, and k_δ = 12.00 ± 2.15 s^{-1}. The magnitudes of k_α and k_δ correspond to the intercept values on the right- and left-hand axes of the plot, respectively. Conditions: phosphate buffer (0.3 M, pH 6.4), $\Gamma/2$ = 1 M, 25 °C.

$k_\alpha k_\gamma$[MTG]/(k_β[S] + k_γ[MTG]); in the reverse direction, k_r = $k_\beta k_\delta$[S]/(k_β[S] + k_γ[MTG]). Since k(obsd) = k_f + k_r

$$k(\text{obsd}) = \frac{k_\alpha k_\delta [R(S_f) + 1 - S_f]}{k_\alpha(1 - S_f) + k_\delta R(S_f)} \qquad (5)$$

where R equals the dissociation equilibrium constant for H

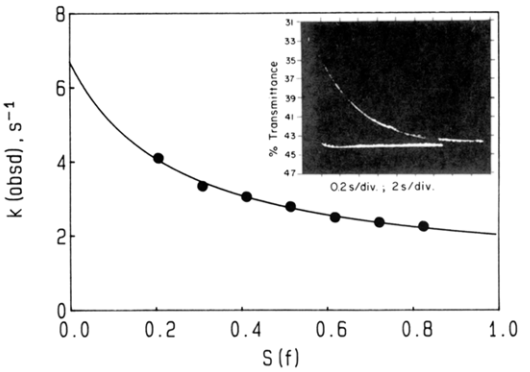

FIGURE 3: Variation of k(obsd) versus S_f for the thiohemiacetals formed from glutathione and methyl thioglycolate with phenylglyoxal. Observed rate constants [k(obsd)] were obtained from the first-order decrease in optical density at 350 nm of the observation chamber, into which one syringe delivered glutathione thiohemiacetal (2.97 mM) plus successively decreasing concentrations of free glutathione (77–17 mM) and the other syringe delivered successively increasing concentrations of methyl thioglycolate (20–80 mM). In each experiment, [glutathione] + [methyl thioglycolate] = 97 mM. The error in the values of k(obsd) is in the range 0.7–1.3%, on the basis of random error in the data points over 3–4 half-lives. The solid line through the data of the figure was calculated from eq 5 in which R is experimentally fixed at 1.52, k_α = 2.02 ± 0.04 s^{-1}, and k_δ = 6.70 ± 0.33 s^{-1}. Conditions: phosphate buffer (0.15 M, pH 6.3), ethylenediaminetetraacetate (2 mM), $\Gamma/2$ = 0.78 M, 25 °C. Inset: Photograph of the stopped-flow kinetic trace at S_f = 0.722. The reaction is first-order over 4 half-lives with a random error of ±0.78%; k(obsd) = 2.36 ± 0.02 s^{-1}.

Table I: Dissociation Constants for the Thiohemiacetals Due to Glutathione (GSH) and to Methyl Thioglycolate (MTG) with Phenylglyoxal as a Function of Ionic Strength and pH[a]

$\Gamma/2$ (M)	pH	K_{diss}(GSH) (mM)	K_{diss}(MTG) (mM)	R^b
0.78	6.3	1.57	1.03	1.52
1.50	6.3	1.84	1.16	1.59
2.20	6.3	1.67	1.15	1.45
0.78	4.6	0.942	0.620	1.52
1.50	4.6	0.935	0.570	1.64
2.00	4.6	0.907	0.570	1.59

[a] For the measurements at pH 6.3 and 4.6, phosphate (0.15 M) and acetate (0.15 M) buffers were used, respectively; 25 °C. [b] R = K_{diss}(GSH)/K_{diss}(MTG). For the determinations at pH 6.3, R(average) = 1.52; for the determinations at pH 4.6, R(average) = 1.58.

divided by that for H′ (1.52) and S_f equals the mole fraction of methyl thioglycolate in the reaction mixture [S_f = [MTG]/([MTG] + [S])]. The microscopic rate constants, k_α and k_δ, were evaluated from the variation of k(obsd) with S_f, wherein k(obsd) = k_α when S_f = 1 and k(obsd) = k_δ when S_f = 0 (Figure 2).

The rate constants for decomposition of H_R and H_S were determined by the same method (Figure 3). That k_1 and k_4 are essentially equivalent is indicated by the observation that systematic deviations from first-order kinetics were *not* observed in any of the individual kinetic runs over 3–4 half-lives. Biphasic kinetics would be expected for two concurrent but unequal first-order processes.[2] Thus, the reaction of eq 4 may be generalized to include the diastereotopic thiohemiacetals (eq 2), with the qualifications that H = H_R + H_S, S = GSH, and k_α = k_1 ≃ k_4. Observed decomposition rate constants,

[2] For example, for the kinetic run shown in Figure 3 (inset) 20 data points were taken over 4 half-lives. The quality of the fit of the data to a single exponential decay in the optical density (k_1 = k_4) becomes approximately equal to that for a double exponential decay [$A_\infty - A_t$ = $0.5(A_\infty - A_t)\exp(-k_1 t) + 0.5(A_\infty - A_t)\exp(-k_4 t)$] when the magnitudes of k_1 and k_4 differ by 20% or less. Therefore, k_1 = k_4 with an estimated error of ~20%.

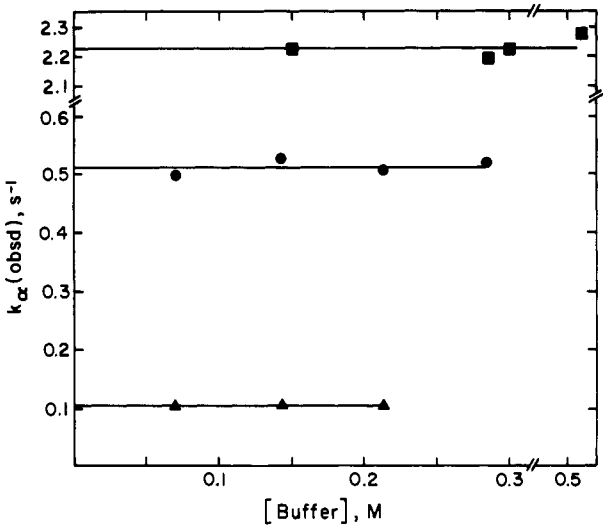

FIGURE 4: Observed dissociation rate constants [k_α(obsd)] for the thiohemiacetal formed from glutathione and phenylglyoxal as a function of [buffer] at different pH: acetate, pH 4.92 (▲), average k_α(obsd) = 0.10; phosphate, pH 5.60 (●), average k_α(obsd) = 0.51; phosphate, pH 6.31 (■), average k_α(obsd) = 2.23; $\Gamma/2$ = 1.43 M, 25 °C. In order to optimize the accuracy of k_α(obsd), four to seven individual kinetic measurements were obtained in the range S_f = 0.84–0.37. [Accurate values of k_δ(obsd) cannot be obtained by using this range of S_f.] The computer best-fit values for k_α(obsd) were obtained by using R = 1.52 for determinations at pH 6.31 and 5.6 and R = 1.58 for determinations at pH 4.92. The error in k_α(obsd) values obtained in phosphate buffer was in the range ±2–5%; in acetate buffer the error was ±3%.

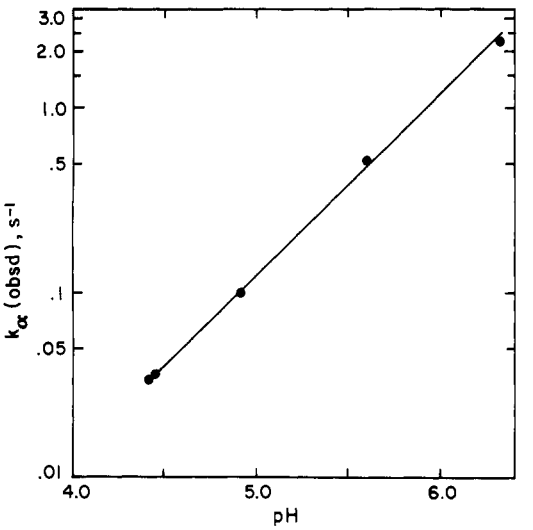

FIGURE 5: Observed dissociation rate constants [k_α(obsd)] for the thiohemiacetal formed from glutathione and phenylglyoxal as a function of pH. Data were taken from the intercepts of the buffer plot, Figure 4. Two additional measurements were made in acetate buffer (0.15 M) at pH 4.42 [k_α(obsd) = 0.033 ± 0.002] and pH 4.45 [k_α(obsd) = 0.036 ± 0.002]; $\Gamma/2$ = 1.43, 25 °C.

k_α(obsd) and k_δ(obsd), under different conditions, were obtained by regression analysis of the kinetic data to eq 5, using experimental values of R that were essentially invariant with pH (4.6–6.3) and ionic strength (0.78–2.2 M) (Table I). Free GSH and free methyl thioglycolate do not appear to catalyze the decomposition of the thiohemiacetals, since the magnitude of k_α(obsd) is independent of the total concentration of these two mercaptans in the reaction mixtures (77–147 mM). Moreover, there is no evidence for general catalysis by either phosphate or acetate (Figure 4). The magnitude of k_α(obsd) is primarily dependent upon hydroxide ion concentration in the pH range 4.4–6.4, where the rate constant for hydrolysis by water is negligible (Figure 5): k_α(obsd) = k_{OH}[OH$^-$], and k_{OH} = (1.14 ± 0.10) × 10^8 M^{-1} s^{-1}. The same has been observed for the decomposition of thiohemiacetals formed from simple aldehydes like acetaldehyde and weakly acidic mercaptans like ethanethiol (k_{OH} = 0.8 × 10^8 M^{-1} s^{-1}; Barnett & Jencks, 1969). Expulsion of the mercaptide ion from the thiohemiacetal is probably rate determining in all of the above processes (Barnett & Jencks, 1969). The larger rate constant for the thiohemiacetal formed from phenylglyoxal and methyl thioglycolate ($k_{OH} \simeq 5 \times 10^8$ M^{-1} s^{-1}) is in keeping with the greater acidity of the leaving group (pK_a 7.3; Barnett & Jencks, 1969). The carboxyl and amino functions of the glutathionyl moiety do not significantly catalyze the decomposition of the thiohemiacetal function, on the basis of the above comparisons. This is in accordance with the absence of terms for general catalysis in the rate law for the decomposition of thiohemiacetals formed from weakly acidic mercaptans.

Direct measurement of the decomposition rate constants for the thiohemiacetals formed from methylglyoxal and GSH would have been most useful, since methylglyoxal is the likely physiological substrate for glyoxalase I. However, this could not be done because there are no significant spectral differences between the thiohemiacetals formed from GSH and from methyl thioglycolate. Nevertheless, the decomposition rate constants for the methylglyoxal and phenylglyoxal thiohemiacetals are probably very similar, since the decomposition rate constants are relatively insensitive to aldehyde structure. This is evidenced by the near identity of k_{OH} for the phenylglyoxal–2-mercaptoethanol and acetaldehyde–ethanethiol thiohemiacetals.

Nonstereospecific Substrate Usage by Glyoxalase I. That H_R and H_S are used by glyoxalase I with roughly equal efficiencies is indicated when the near equivalence of k_1 and k_4 is taken together with the results of previously published isotope-trapping experiments (Griffis et al., 1983). The isotope-trapping experiments emphasized that both H_R and H_S are used as substrates by the enzyme and were consistent with equal rates of usage of the two diastereomers. However, the error in the data obtained by this method could potentially accommodate k_{cat}/K_m values for H_R and H_S that differ by a factor of about 2 and about 5 for porcine erythrocyte and yeast glyoxalase I, respectively. More seriously, the isotope-trapping method could not exclude the possibility that unequal values of k_{cat}/K_m for the diastereomers were concealed by unequal values of k_1 and k_4. The latter possibility is now unlikely on the basis of the results of the stopped-flow experiments. It should be emphasized, however, that H_R and H_S may not be used with identical efficiencies, in view of the report that the resonances due to H_R and H_S are lost at different rates in D_2O solvent (pD 4.4) in the presence of yeast glyoxalase I (Brown et al., 1981).

Kinetic Model. The minimum kinetic scheme for the conversion of methylglyoxal to D-lactate in cells is shown at the bottom of Figure 6. The symbol H_{R+S} represents the *sum* of the diastereotopic thiohemiacetals H_R and H_S. Both diastereomers are assumed to be directly used by glyoxalase I with approximately equal k_{cat}/K_m efficiencies, on the basis of the results described above. The rate constants of Figure 6 and eq 2 are related as follows: The rate constant $k_7 = k_1 \simeq k_4$, since d[M]/dt = $k_1[H_R] + k_4[H_S]$, where $k_1 \simeq k_4$; $k_8 = k_2 + k_3$, since d($H_R + H_S$)/dt = $(k_2 + k_3)$[GSH][M]. Moreover, $k_2 \simeq k_3$, since $k_1 \simeq k_4$ and $[H_R] \simeq [H_S]$ at equilibrium. The near equality of $[H_R]$ and $[H_S]$ is shown by the near-equal integrated intensities of the resonances due to the diastereotopic thiohemiacetal protons arising from GSH (20 mM) and me-

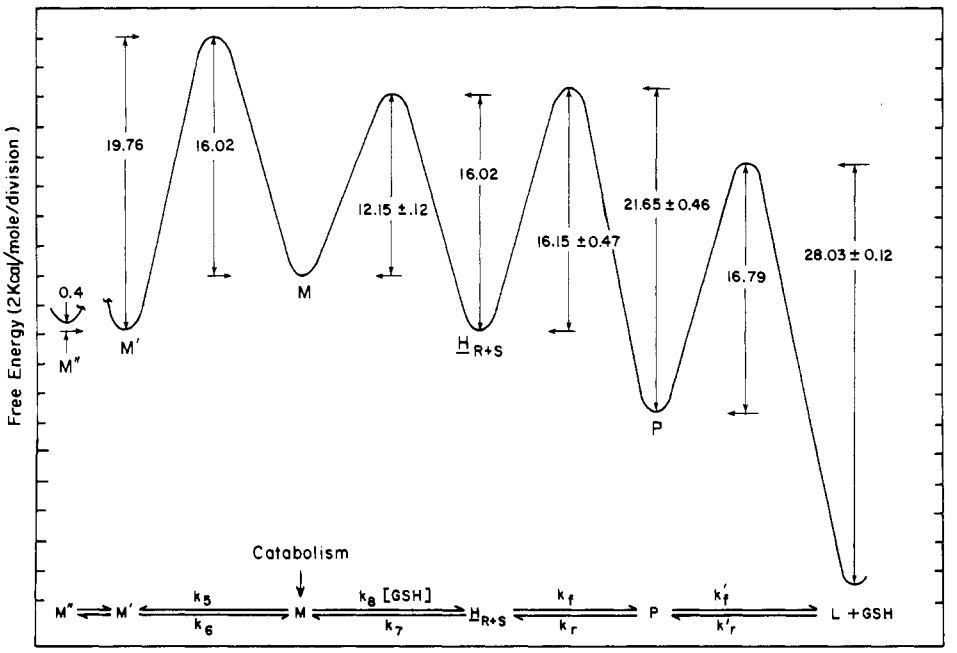

FIGURE 6: Kinetic scheme and free energy diagram for the catabolism of methylglyoxal in mammalian erythrocytes where M = methylglyoxal; M′ and M″ = mono- and dihydrates of methylglyoxal, respectively; $H_{R+S} = H_R + H_S$; P = (*S*)-D-lactoylglutathione; and L = D-lactate. The ΔG and $\Delta G^{\ddagger}$ values were calculated for the rate (k) and equilibrium (K_{eq}) constants given in Table II by using the relationships $K_{eq} = \exp(-\Delta G/RT)$ and $k = (k'T/h)\exp(-\Delta G^{\ddagger}/RT)$, where k' = Boltzmann's constant, T = 298 K, h = Planck's constant, and R = the gas constant.

Table II: Magnitudes of the Rate and Equilibrium Constants for the Kinetic Scheme of Figure 6[a]

equilibrium constants	associated rate constants
Nonenzymic Reactions	
$K''_h = [M'']/[M'] \simeq 0.5$	not known
$K'_h = [M']/[M] = 565$	$k_5 \simeq 11\ s^{-1}$
	$k_6 \simeq 0.02\ s^{-1}$
$K_S = [H_{R+S}]/([M][GSH]) =$	$k_7 \simeq 11\ s^{-1}$
$2.8 \times 10^5\ M^{-1}$	$k_8 \simeq 3.1 \times 10^6\ M^{-1}\ s^{-1}$
	$[k_8[GSH] \simeq (6.2\text{–}9.3) \times 10^3\ s^{-1}]^c$
Enzymic Reactions	
$K_{eq} = [P]/[H_{R+S}] = 1.1 \times 10^4$	$k_f^d \simeq 4\text{–}20\ s^{-1}$
	$k_r^d \simeq (3.6\text{–}18) \times 10^{-4}\ s^{-1}$
$K'_{eq} = [L][GSH]/[P] \simeq$	$k'^e_f \simeq 3\ s^{-1}$
$4.4 \times 10^5\ M$	$k'^e_r \simeq 6.8 \times 10^{-6}\ M^{-1}\ s^{-1}$
$[[L]/[P] = (1.5\text{–}2.2) \times 10^8]^b$	$[k'_r[GSH] \simeq (1.4\text{–}2.0) \times 10^{-8}\ s^{-1}]^c$

[a] The methods used to obtain these constants are given in the text. [b] Apparent equilibrium constant for $[GSH]_{free}$ = 2–3 mM. [c] Pseudo-first-order rate constant for $[GSH]_{free}$ = 2–3 mM. [d] Range of apparent rate constants equal to $k_{cat}E_t/K_m$ for glyoxalase I in erythrocytes (pig, rat, human) (Table III). [e] Apparent rate constant equal to $k_{cat}E_t/K_m$ for glyoxalase II in rat erythrocytes (Table III).

thylglyoxal (20 mM), in D_2O solvent (32 °C): δ 5.579 (0.53H), 5.560 (0.47H) versus DSS; pD $\simeq$ 4 (80 MHz).

The free energy diagram of Figure 6 illustrates the relative kinetic importance of the various steps in the reaction scheme for mammalian erythrocytes and was calculated from the apparent rate constants listed in Table II. These rate constants apply when $[GSH]_t \simeq [GSH]_{free} \simeq$ 2–3 mM and were deduced on the basis of the reasoning given below. The apparent rate constants for the reactions catalyzed by glyoxalases I (k_f, k_r) and II (k'_f, k'_r) apply when the concentrations of H_{R+S} and P are small in comparison to the K_m's for these enzymes (Table III). Erythrocytes were chosen as a model cell system because (a) they are relatively simple and uncompartmentalized in comparison to other cell types, (b) the intracellular concentrations of GSH have been carefully established (2–3 mM) in different mammalian systems, and (c) the kinetic properties and intracellular concentrations of the glyoxalase enzymes in erythrocytes can be estimated with fair accuracy. The kinetic model is simplified by the absence of any evidence for allosteric control of the glyoxalase enzymes.

Assumptions. Quantitation of the rate constants in the kinetic model depends upon four fundamental assumptions: (1) The enzyme and substrate molecules within the cell are assumed to be freely diffusible; the kinetic properties of the glyoxalase enzymes are taken to be identical with those determined on the basis of in vitro measurements. (2) The decomposition rate of H_{R+S} is assumed to depend only upon the pH of the intracellular space. This assumption is supported by the observation that the decomposition rate of GSH–(*R*,*S*)-phenylglyoxal thiohemiacetal is specific base catalyzed and is insensitive to buffer ion concentration. (3) Methylglyoxal and GSH are assumed *not* to separately serve as substrates for glyoxalase I. This is supported by the results of two published studies in which conditions could *not* be found that would allow the glyoxalase I reaction to proceed faster than the rate of formation of H_{R+S} from methylglyoxal and GSH (Vander Jagt et al., 1975; Marmstal & Mannervik, 1981). (4) The glyoxalase pathway is assumed to provide the only means for removing methylglyoxal from erythrocytes. In apparent contradiction to this assumption, the ubiquitous enzyme formaldehyde dehydrogenase has been reported to efficiently use methylglyoxal as an alternate substrate, thus providing a competing route for the removal of methylglyoxal from cells. However, recent kinetic and product analysis studies on the dehydrogenases from both cow and human liver indicate that the enzyme is highly specific for formaldehyde (Pourmotabbed & Creighton, 1986). Past reports that methylglyoxal is a substrate for the dehydrogenase can be explained on the basis of the demonstrated presence of contaminating formaldehyde in some commercial preparations of methylglyoxal. Also, crude preparations of a 2-oxoaldehyde dehydrogenase activity have been reported to catalyze the $NAD(P)^+$-dependent oxidation of methylglyoxal to pyruvate (Monder, 1967). However, unlike glyoxalase I, this enzyme activity is highly organ specific as well as species specific (rat liver; sheep kidney, lung, and adrenal); no such activity has been reported to be present in erythrocytes.

Table III: Activity of Glyoxalases I and II in Erythrocytes Freshly Obtained from Different Mammalian Sources

source	assay conditions	act.[a] (units/mL)	K_m (mM)	$k_{cat}E_t/K_m$[b] (s^{-1})
Glx I:				
pig[c]	imidazole hydrochloride (25 mM); pH 7 (25 °C)	63 ± 9	0.14[d]	7.5 ± 1.1
pig[e]	imidazole hydrochloride (25 mM); pH 7 (30 °C)	54	0.14[d]	6.4
rat[f]	phosphate (44 mM), KCl (0.1 M), $MgCl_2$ (10 mM); pH 7 (25 °C)	114	0.09	21.1
human[g]	imidazole hydrochloride (25 mM); pH 7 (30 °C)	58	0.13	7.4
human[h]	phosphate (44 mM), KCl (0.1 M); pH 7 (25 °C)	26	0.12	3.6
Glx II:				
rat[i]	Tris (50 mM); pH 7.4 (25 °C)	~34	0.18[j]	~3.1

[a] Defined as micromoles of (*S*)-D-lactoylglutathione formed per minute per milliliter of packed erythrocytes under maximum velocity conditions. [b] Calculated as being equal to (activity)/[K_m × (60 s/min)]. [c] This work. The reported activity is the average value and range of values obtained from three separate determinations on the same sample of whole pig blood. [d] Taken from Griffis et al. (1983). [e] Based upon the work of Aronsson and Mannervik (1977). Activity under maximum velocity conditions was calculated from their reported activity (34 units/mL) obtained under assay conditions in which the GSH(*R*,*S*)methylglyoxal thiohemiacetal concentration would have been ~0.24 mM, on the basis of $[GSH]_t$ = 0.66 mM, $[methylglyoxal]_t$ = 2 mM, and an association constant for the thiohemiacetal of 333 M^{-1} (Vander Jagt et al., 1972). [f] Based upon the work of Han et al. (1976). The activity per milliliter of packed erythrocytes was calculated on the basis of their reported units of activity per milliliter of whole blood (49 units/mL) and a hematocrit of 0.43 (Sanderson & Phillips, 1981). [g] Based upon the work of Aronsson et al. (1979). Activity under maximum velocity conditions was calculated on the basis of the correction described in footnote *e*. [h] Based upon the work of Schimandle and Vander Jagt (1979) on the Glo 2-1 allozyme. The activity per milliliter of packed erythrocytes was calculated on the basis of their reported units of activity per milliliter of whole blood (11.8 units/mL) and a hematocrit of 0.45 (Sanderson & Phillips, 1981). [i] Taken from Ball and Vander Jagt (1979). [j] Taken from Ball and Vander Jagt (1981).

Nonenzymic Reactions. The magnitudes of the rate and equilibrium constants for the nonenzymic reactions of Figure 6 were obtained as follows:

The magnitude of k_7 was calculated for pH 7 from the rate law $k_7 = 1.1 \times 10^8\ M^{-1}\ s^{-1}\ [OH^-]$ which applies for the decomposition of GSH–(*R*,*S*)-phenylglyoxal thiohemiacetal down to at least pH ≃ 4.4.

The magnitude of k_8 was ultimately obtained from the definition

$$K_S = [H_{R+S}]/([GSH][M]) = k_8/k_7 \qquad (6)$$

The magnitude of K_S is related to experimentally obtainable parameters by

$$K_S = K_S^{obsd}(1 + K_h) \qquad (7)$$

where $K_S^{obsd} = [H_{R+S}]/[[GSH]([M] + [M'] + [M''])] = 333 \pm 70\ M^{-1}$ [phosphate buffer (67 mM, pH 7), Γ/2 = 0.2 M; Vander Jagt et al., 1972], and $K_h = ([M'] + [M''])/[M]$. The hydration constant (K_h) is a large number, since aldehydic proton resonances are not apparent in D_2O solutions of methylglyoxal. Nevertheless, the magnitude of K_h can be obtained from the equality

$$K_h = K'_h(1 + K''_h) \qquad (8)$$

where $K'_h = [M']/[M]$ and $K''_h = [M'']/[M']$. K'_h was estimated from the Hammett–Taft correlation $\log K_h^\circ \simeq 1.68\delta^* - 0.02$, derived from the hydration constants for seven different aliphatic aldehydes spanning the range $K_h^\circ = 1.4–(2.78 \times 10^4)$ (Greenzaid et al., 1967); therefore, $K_h^\circ = K'_h \simeq 565$ when $\delta^* = 1.65$ for the substituent $H_3CC{=}O$ (Taft, 1957). Moreover, $K''_h \simeq 0.5$, on the basis of the relative equilibrium distribution of M′ and M″ in D_2O solvent determined by NMR (Figure 7). Therefore, $K_h \simeq 848$ (eq 8), $K_S \simeq 2.8 \times 10^5\ M^{-1}$ (eq 7), and $k_8 \simeq 3.1 \times 10^6\ M^{-1}\ s^{-1}$ (eq 6). The range for the maximum value of k_8[GSH] was calculated on the basis of intracellular [GSH] = 2–3 mM determined for human, rat, and sheep erythrocytes (Kosower & Kosower, 1978).

The magnitude of k_6 was obtained from the reported initial velocity (v_i) of thiohemiacetal formation (monitored spectrophotometrically) from methylglyoxal (5 mM) and GSH under conditions where v_i is independent of the concentration of GSH (0.5–5.0 mM), presumably because dehydration of methylglyoxal is rate determining: $v_i = (1.6 \pm 0.2) \times 10^{-5}\ M\ s^{-1}$, in phosphate buffer (44 mM) and KCl (0.1 M), pH 7, 5 °C

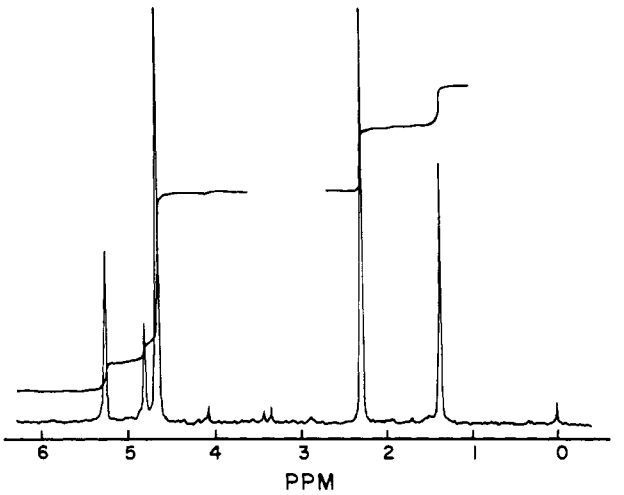

FIGURE 7: H1-80-MHz NMR spectrum of methylglyoxal in D_2O. Aldehydrol: δ 2.31 (3 H), 5.27 (1 H). Dihydrate of methylglyoxal: δ 1.38 (3 H), 4.82 (1 H). HOD: δ 4.65. From the integrated intensities of the resonances, [aldehydrol]/[dihydrate] ≃ 2. Reference standard, DSS.

(Vander Jagt et al., 1975). The fact that the same initial velocity was observed by including high concentrations of glyoxalase I in this system and following thioester product formation suggests that the dehydration of M′, and not M″, is reflected in v_i:

$$\underset{M'}{CH_3C(=O)CH(OH)OH} \xrightarrow{k_6} H_2O + CH_3C(=O)C(=O)H \xrightarrow[(Glx\ I)]{GSH} P \qquad (9)$$

Moreover, this observation suggests that glyoxalase I does not catalyze the dehydration of M′. Therefore, $v_i = k_6[M']$. Assuming that v_i increases ~2-fold per 10 °C rise in temperature, k_6 (25 °C) ≃ $4(1.6 \times 10^{-5}\ M\ s^{-1})/(0.67)(5 \times 10^{-3}\ M) \simeq 0.02\ s^{-1}$. Since $K'_h = k_5/k_6$, $k_5 \simeq 11\ s^{-1}$.

There are two potential sources of uncertainty in using the above values of k_5 and k_6 to estimate the rate of the hydration equilibrium for methylglyoxal in erythrocytes. The first is that intracellular carbonic anhydrase may catalyze the hydration equilibrium, by virtue of its demonstrated ability to catalyze the reversible hydration of simple aromatic and aliphatic aldehydes (Pocker & Meany, 1965). However, the results of a recent study seem to preclude this possibility. While phe-

nylglyoxal is a poor substrate for carbonic anhydrase, no detectable activity could be found with methylglyoxal (Marmstal & Mannervik, 1981). A second source of uncertainty is that intracellular buffer ions may catalyze the hydration equilibrium. The hydration of simple aldehydes is subject to general acid–base catalysis (Funderburk et al., 1978; Bell & Evans, 1966). The major buffer species in human erythrocytes, other than intracellular proteins, are bicarbonate (~20 mM), phosphate (~5 mM), ATP (~12 mM), and diphosphoglycerate (~35 mM) (Guest, 1942). However, we believe that general catalysis by intracellular buffer ions is unlikely to give rise to a hydration rate that is dramatically different from that determined in phosphate buffer (44 mM, pH 7). Therefore, the essential conclusion that $k_5 \ll k_8[GSH]$ is probably still valid within the cell. In any event, we propose the above values for k_5 and k_6 as the best estimates available at this time.

Enzymic Reactions. For the glyoxalase I reaction, a range for k_f ($=k_{cat}E_t/K_m$) was calculated from the V_{max} units of enzyme per milliliter of centrifugally packed pig, rat, and human erythrocytes (Table III). Human erythrocytes reportedly contain three isozyme forms of glyoxalase I (Aronsson et al., 1979). However, the isozymes are kinetically indistinguishable (Schimandle & Vander Jagt, 1979). The range of k_r was calculated by using the Haldane relationship: $K_{eq} = [P]/[H_{R+S}] = k_f/k_r = 1.1 \times 10^4$ (sodium phosphate, 100 mM, pH 7) (Sellin & Mannervik, 1983).

For the glyoxalase II reaction, k'_f ($=k_{cat}E_t/K_m$) was calculated by using the single available literature value for the activity of the enzyme in rat erythrocytes (Table III). The magnitude of this rate constant corresponds to an $\sim 10^6$-fold increase over the rate constant for spontaneous hydrolysis of (*S*)-D-lactoylglutathione, calculated for pH 7 [$k = (9.86 \pm .06) \times 10^{-7}$ s^{-1}] from the observed rate constant obtained from a duplicate determination at pH 8.1 [$k = (1.25 \pm 0.01) \times 10^{-5}$ s^{-1}, argon-saturated sodium pyrophosphate (50 mM)/NaCl, $\Gamma/2 = 0.5$ M, ethylenediaminetetraacetate (0.25 mM), 25 °C] assuming that the hydrolysis reaction is specific base catalyzed (Jencks et al., 1960). An *approximate* value for k'_r was obtained from the approximation $K_{eq} = [L][GSH]/[P] = k'_f/k'_r \simeq 4.4 \times 10^5$ M. The magnitude of the equilibrium constant was, in turn, obtained from the free energy of hydrolysis in dilute aqueous solutions (pH 7) of thioesters of acetic acid, $\Delta G = 7.7$ kcal/mol (Jencks et al., 1960).

Discussion

Evaluation of the rate constants of Figure 6 provides a unique opportunity to assess the probable kinetic factors controlling the chemical removal of methylglyoxal from cells. Of greater general importance is the additional opportunity to evaluate how well the glyoxalase pathway is adapted to this purpose. In several respects, the efficiency of the pathway is governed by the same thermodynamic principles that probably determine the catalytic efficiencies of individual enzyme molecules (Albery & Knowles, 1976a).

Limitations on Efficiency. The rate of conversion of methylglyoxal to D-lactate will be limited by different factors depending upon the steady-state concentrations of intermediates in the pathway: $[M]_{ss}$, $[GSH]_{ss}$, $[H_{R+S}]_{ss}$, and $[P]_{ss}$. Since these concentrations are not known experimentally, two general cases are considered:

Case I: $[H_{R+S}]_{ss}$, $[P]_{ss} \ll K_m$'s. Under conditions where the steady-state concentrations of metabolites are small in comparison to the K_m values for glyoxalases I ($K_m \simeq 0.1$ mM) and II ($K_m \simeq 0.2$ mM), the apparent rate constants for the enzyme-catalyzed steps reduce to $k_{cat}E_t/K_m$, and $[GSH]_t \simeq [GSH]_{ss}$. There are good reasons to believe that many intracellular enzymes which do not occupy control points in metabolism operate under conditions where [substrate] $< K_m$, as discussed by Albery and Knowles (1976a). For example, this is true for several of the glycolytic enzymes (Hess, 1973).

The free energy diagram of Figure 6 illustrates the relative kinetic importance of the enzymic and nonenzymic barriers to the conversion of methylglyoxal to D-lactate under these conditions. The hydration of methylglyoxal is kinetically unimportant, since the apparent rate constant for formation of H_{R+S} ($k_8[GSH]_t$) is (~500–10^3)-fold larger than the rate constant for hydration (k_5); the overall thermodynamic barrier to formation of D-lactate from methylglyoxal is small in comparison to that for hydration. Therefore, the steady-state rate of appearance of D-lactate ($v = dL/dt$) will conform to eq 10, derived on the basis of the following equations and

$$v = k_{catp}[GSH]_t[M]_{ss}/(K_{mp} + [M]_{ss}) \qquad (10)$$

approximations: $d[L]/dt = k'_f[P]_{ss}$; $d[P]_{ss}/dt = k_f[H_{R+S}]_{ss} - (k_r + k'_f)[P]_{ss} \simeq 0$; $d[H_{R+S}]_{ss}/dt = k_8[GSH]_{ss}[M]_{ss} + k_r[P]_{ss} - (k_f + k_7)[H_{R+S}]_{ss} \simeq 0$; $[GSH]_t = [GSH]_{ss} + [H_{R+S}]_{ss} + [P]_{ss}$; and $k'_r \simeq 0$. In eq 10

$$k_{catp} = \frac{k'_f k_f}{k'_f + k_r + k_f} \simeq 1.7\text{–}2.6 \text{ s}^{-1}$$

$$K_{mp} = \frac{k_7 k_r + k'_f(k_7 + k_f)}{k_8(k'_f + k_r + k_f)} \simeq 1.3\text{–}2.1 \ \mu\text{M}$$

The form of eq 10 is identical with that of the Michaelis–Menten equation. However, under the conditions of case I, $[M]_{ss} \ll K_{mp}$ since $[GSH]_t \simeq [GSH]_{ss}$ and $K_{mp}/[M]_{ss} = [GSH]_{ss}/[[P]_{ss} + [H_{R+S}]_{ss}]$. The latter equality is analogous to that for an enzymic reaction in which $K_m/[\text{substrate}] = [\text{enzyme}]/\sum[\text{enzyme-bound substrate forms}]$ (Fersht, 1977). Thus, eq 10 reduces to

$$v = (k_{catp}/K_{mp})[GSH]_t[M]_{ss} \qquad (11)$$

The efficiency of the glyoxalase pathway may be defined in terms of an efficiency function (E_f) where

$$E_f = v/v_m \qquad (12)$$

and $v_m = k_8[GSH]_t[M]_{ss}$. This function reflects how closely the velocity of the pathway approaches the limiting bimolecular rate of addition of GSH to methylglyoxal (v_m), a process that the cell apparently is unable to control. Hence, maximum efficiency ($E_f = 1$) is achieved when the enzyme-catalyzed steps are so rapid that the rate of formation of H_{R+S} is the rate-determining step in the pathway; i.e., $v = v_m$. On this basis, the actual efficiency of the pathway is ~50% of maximal, using the numerical values of k_{catp} and K_{mp} in eq 13,

$$E_f = k_{catp}/(K_{mp}k_8) \simeq 0.5 \qquad (13)$$

obtained by combining eq 11 and 12. This analysis is similar to that used for evaluating the efficiency of an enzyme, wherein the magnitude of k_{cat}/K_m is compared with the estimated magnitude of the bimolecular rate constant for diffusion-controlled encounter of substrate and active site. In this sense, the efficiency of the glyoxalase pathway parallels that of the well-studied triosephosphate isomerase reaction, on the basis of an analogous efficiency function ($E_f \simeq 0.6$) that reflects the degree to which the diffusional step is rate determining when [substrate] $\ll K_m$ (Albery & Knowles, 1976a).

However, there is an additional aspect to efficiency in a metabolic pathway that is not readily apparent from the magnitude of E_f. From the standpoint of cellular energetics, the benefit to the cell of increasing E_f must be balanced against

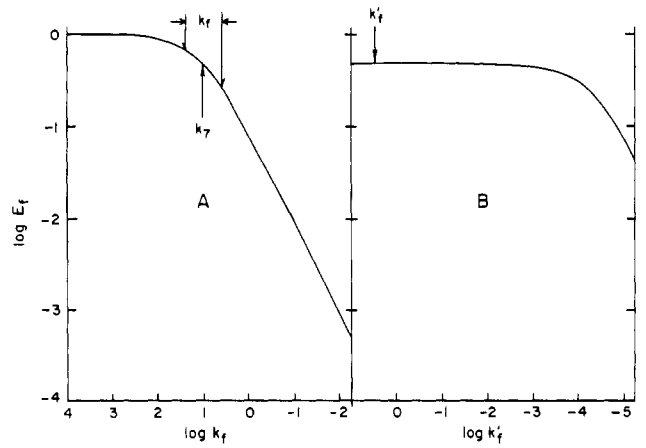

FIGURE 8: Log plot of the variation of E_f versus k_f (panel A) and versus k'_f (panel B) according to eq 14. The solid lines were calculated by varying either k_f or k'_f and keeping the other constants fixed at the values shown in Table II. For the variation of E_f versus k'_f, a value of 10 s^{-1} was used for k_f.

the energy expended in order to synthesize enzyme protein. The concentration of glyoxalase I in erythrocytes seems to reflect such a balance. The apparent rate constant for enzyme-catalyzed conversion of H_{R+S} to P ($k_f \simeq 4$–20 s^{-1}) is approximately equal to the decomposition rate constant for H_{R+S} ($k_7 = 11$ s^{-1}, pH 7). Therefore, the concentration of glyoxalase I is just that necessary in order to lower the top of the free energy barrier for catalysis to that for the interconversion of H_{R+S} and GSH plus methylglyoxal. The synthesis of more enzyme in order to further reduce the catalytic barrier would result in only small increases (no more than 2-fold) in the apparent rate constant for conversion of methylglyoxal plus GSH to P. This phenomenon is graphically illustrated by the log plot of Figure 8 showing the variation of E_f versus k_f according to the following equation, obtained by combining eq 13 with the kinetic definitions of k_{catp} and K_{mp} (eq 10):

$$E_f = k'_f/(k_7/K_{eq} + k'_f k_7/k_f + k'_f) \qquad (14)$$

where

$$K_{eq} = k_f/k_r \qquad \text{(Table II)}$$

All of the experimental values for k_f (Table II) fall near the "break point" in efficiency centered about k_7.

A similar analysis for glyoxalase II reveals that k'_f is $\sim 10^4$ times larger than the break point in efficiency near k_r (Figure 8). This means that the cell contains $\sim 10^4$ times more glyoxalase II than is necessary for near-maximal efficiency of the pathway when $[M]_{ss} \ll K_{mp}$. However, there is a reasonable explanation for the apparent excess of glyoxalase II in the cell. If indeed the concentration of this enzyme were such that $k'_f \simeq k_r$, K_{mp} would decrease by a factor of roughly 10^3. This, in turn, would increase the chances that $[M]_{ss} > K_{mp}$. Under these conditions, most of the GSH in the cell is converted to P_{ss} and the velocity of the pathway is now limited by the small number of units of glyoxalase II (see below). Indeed, the amount of glyoxalase II in the cell is roughly that necessary ($k'_f \simeq k_f$) in order to *increase* K_{mp} to within a factor of 2 [$K_{mp} \simeq (k_7 + k_f)/2k_8$] of the theoretical maximum [when $k'_f \gg k_f$, $K_{mp} \simeq (k_7 + k_f)/k_8$] for the amount of glyoxalase I in the cell (Figure 9).

Case II: $[H_{R+S}]_{ss}$, $[P]_{ss} \gg K_m$'s. Clearly, the rate of formation of D-lactate cannot exceed the V_{max} units ($k_{cat}E_t$) of glyoxalase II in the cell. This upper limit would be reached under conditions where the flux through the pathway is sufficiently high ($[M]_{ss} \geq K_{mp}$) so that the concentrations of intermediary metabolites are large in comparison to the K_m's of the glyoxalase enzymes. In this concentration range, v is bounded by $k_{cat}E_t$ for glyoxalase II, and E_f becomes $\ll 1$ (eq. 12).

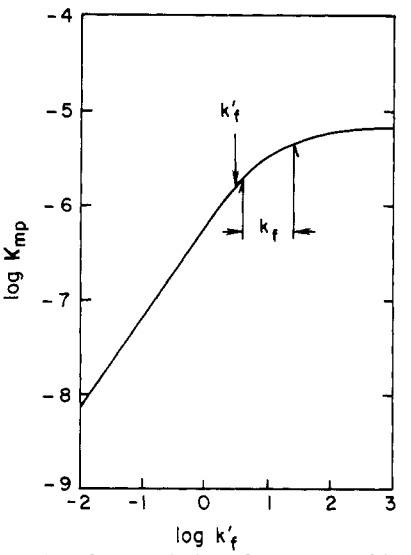

FIGURE 9: Log plot of the variation of K_{mp} versus k'_f according to the kinetic definition of K_{mp} (eq 10). The solid line was calculated by varying k'_f and keeping the other constants fixed at the values shown in Table II; a value of 10 s^{-1} was used for k_f.

Substrate Specificity of Glyoxalase I. The capacity of glyoxalase I to use both diastereotopic thiohemiacetals (H_{R+S}) with nearly equal k_{cat}/K_m efficiencies enhances the overall efficiency of the glyoxalase pathway under case I conditions. If only one of the diastereomers were used by the enzyme (say, H_R), the apparent rate constant for conversion of both diastereomers to P must contain k_7 since $k_{app} = 0.5k_7/(1 + k_7/k_f)$, where $0.5k_7$ is the apparent rate constant for interconversion of the diastereomers when $k_1 \simeq k_4$:

$$H_S \underset{0.5k_7}{\overset{0.5k_7}{\rightleftharpoons}} H_R \xrightarrow{k_f} P \qquad (15)$$

In the nonstereospecific case, $k_{app} = k_f$. Therefore, the kinetic advantage of nonstereospecific substrate usage by the enzyme is $2[(k_7 + k_f)/k_7] \simeq 3$–$6$, on the basis of the range of k_f values in Table II.

However, the substrate specificity of glyoxalase I seems less than optimal in view of the fact that H_{R+S} alone serve as substrates for the enzyme. This means that the velocity of the pathway is primarily limited by the rate of addition of GSH to methylglyoxal ($k_8[GSH]_t$) under case I conditions (Figure 6). In principle, this limitation could be overcome, if the enzyme had the additional ability to use GSH and methylglyoxal directly. However, a change in substrate specificity alone would not increase the velocity of the pathway, since the thermodynamic barrier for the glyoxalase I reaction (~ 16 kcal) is substantially greater than that for formation of H_{R+S} (~ 12 kcal); i.e., $k_f \ll k_8[GSH]_t$. Either one or both of two strategies would have to be employed in order for $k_f > k_8[GSH]_t$: Either the cell must synthesize more enzyme and/or the catalytic efficiency (k_{cat}/K_m) of the enzyme must increase so that k_f increases by (>500–10^3)-fold. Clearly, the former strategy involves the disadvantageous expenditure of more ATP by the cell. With respect to the latter strategy, it may not be possible to improve k_{cat}/K_m by a factor of >500–10^3, since glyoxalase I is already a highly efficient catalyst for H_{R+S}. The enzyme from yeast obeys Briggs–Haldane kinetics for which $k_{cat}/K_m = 3.5 \times 10^6$ M^{-1} s^{-1} for phenylglyoxal

thiohemiacetal (Vander Jagt & Han, 1973); for the enzyme from human erythrocytes, $k_{cat}/K_m = 1 \times 10^7$ M^{-1} s^{-1} per subunit for methylglyoxal thiohemiacetal (Sellin & Mannervik, 1983). These efficiencies are only 69- and 24-fold smaller than that of the "diffusion-controlled" triosephosphate isomerase reaction, for which $k_{cat}/K_m = 2.4 \times 10^8$ M^{-1} s^{-1} for unhydrated glyceraldehyde 3-phosphate (Albery & Knowles, 1976b). Therefore, the experimentally observed substrate specificity of glyoxalase I may well be optimal when *both* the kinetic and the bioenergetic aspects of the glyoxalase pathway are considered. That the cell would have evolved a separate enzyme to catalyze the formation of H_{R+S} seems unlikely, on the basis of the same reasoning.

Applicability to Other Cell Types. While the efficiency of the glyoxalase pathway in mammalian erythrocytes is near optimal, the efficiency and/or K_{mp} of the pathway in other cell types appears to be somewhat variable. The ratio of the concentrations of glyoxalase enzymes in the crude tissue homogenates obtained from the same organ (liver, kidney, heart, brain, pancreas, muscle, and spleen) among 12 different mammalian species varies in the range 3–30 (Jerzykowski et al., 1978). In addition, the ratio of glyoxalase I/glyoxalase II is variable. For example, in human liver this ratio is ~0.2; in rat muscle the ratio is ~32. Many neoplastic tissues contain substantial amounts of glyoxalase I, but reduced or undetectable amounts of glyoxalase II (Jerzykowski et al., 1975, 1978). Thus, the metabolism of methylglyoxal in many normal and neoplastic tissues may indeed prove to be controlled by a complex interplay of several factors. The quantitative kinetic model proposed here for erythrocytes should serve as a useful starting point for understanding the metabolism of methylglyoxal in more complex tissue types.

Conclusion. The kinetic and thermodynamic factors controlling the efficiency of the glyoxalase pathway in erythrocytes recapitulate those that probably control the catalytic efficiencies of individual enzyme molecules. The pathway seems optimally designed when viewed as a compromise between the opposing factors of (a) maximization of rate at low steady-state levels of intermediary metabolites and (b) minimization of energy expended to synthesize enzyme protein.

ACKNOWLEDGMENTS

We thank Professor Ralph M. Pollack for a helpful discussion and Dr. Angela Wandinger for determining the concentration of glyoxalase I in porcine erythrocytes.

REFERENCES

Albery, W. J., & Knowles, J. R. (1976a) *Biochemistry 15*, 5631.

Albery, W. J., & Knowles, J. R. (1976b) *Biochemistry 15*, 5627.

Alexander, N. M., & Boyer, J. L. (1971) *Anal. Biochem. 41*, 29.

Alger, J. R., & Prestegard, J. H. (1977) *J. Magn. Reson. 27*, 137.

Aronsson, A.-C., & Mannervik, B. (1977) *Biochem. J. 165*, 503.

Aronsson, A.-C., Tibbelin, G., & Mannervik, B. (1979) *Anal. Biochem. 92*, 390.

Ball, J. C., & Vander Jagt, D. L. (1979) *Anal. Biochem. 98*, 472.

Ball, J. C., & Vander Jagt, D. L. (1981) *Biochemistry 20*, 899.

Barnett, R. E., & Jencks, W. P. (1969) *J. Am. Chem. Soc. 91*, 6758.

Bell, R. P., & Evans, P. G. (1966) *Proc. R. Soc. London, A 291*, 297.

Brouwer, A. C., & Kirsch, J. F. (1982) *Biochemistry 21*, 1302.

Brown, C., Douglas, K. T., & Ghobt-Sherif, J. (1981) *J. Chem. Soc., Chem. Commun.*, 944.

Browne, C. A., Campbell, I. D., Kiener, P. A., Phillips, D. C., Waley, S. G., & Wilson, I. A. (1976) *J. Mol. Biol. 100*, 319.

Campbell, I. D., Jones, R. B., Kiener, P. A., & Waley, S. G. (1979) *Biochem. J. 179*, 607.

Együd, L. G., & Szent-Györgyi, A. (1966) *Proc. Natl. Acad. Sci. U.S.A. 56*, 203.

Ekwall, K., & Mannervik, B. (1973) *Biochim. Biophys. Acta 297*, 297.

Fersht, A. (1977) *Enzyme Structure and Mechanism*, Freeman, San Francisco.

Funderburk, L. H., Aldwin, L., & Jencks, W. P. (1978) *J. Am. Chem. Soc. 100*, 5444.

Grassetti, D. R., & Murray, J. F., Jr. (1967) *Arch. Biochem. Biophys. 119*, 41.

Greenzaid, P., Luz, Z., & Samuel, D. (1967) *J. Am. Chem. Soc. 89*, 749.

Griffis, C. E. F., Ong, L. H., Buettner, L., & Creighton, D. J. (1983) *Biochemistry 22*, 2945.

Guest, G. M. (1942) *Am. J. Dis. Child. 64*, 401.

Han, L.-P. B., Davison, L. M., & Vander Jagt, D. L. (1976) *Biochim. Biophys. Acta 445*, 486.

Hess, B. (1973) *Symp. Soc. Exp. Biol. 27*, 105.

Hine, J., & Koser, G. F. (1971) *J. Org. Chem. 36*, 3591.

Jencks, W. P., Cordes, S., & Carriuolo, J. (1960) *J. Biol. Chem. 235*, 3608.

Jerzykowski, T., Winter, R., Matuszewski, W., & Szczurek, Z. (1975) *Experientia 31*, 32.

Jerzykowski, T., Winter, R., Matuszewski, W., & Piskorska, D. (1978) *Int. J. Biochem. 9*, 853.

Kosower, N. S., & Kosower, E. M. (1978) *Int. Rev. Cytol. 54*, 109.

Marmstal, E., & Mannervik, B. (1981) *FEBS Lett. 131*, 301.

Monder, C. (1967) *J. Biol. Chem. 242*, 4603.

Needham, J., & Lehmann, H. (1937) *Biochem. J. 31*, 1913.

Penninckx, M. J., Jaspers, C. J., & Legrain, M. J. (1983) *J. Biol. Chem. 258*, 6030.

Pocker, Y., & Meany, J. E. (1965) *Biochemistry 4*, 2535.

Pourmotabbed, T., & Creighton, D. J. (1986) *J. Biol. Chem. 261*, 14240.

Richard, J. P. (1984) *J. Am. Chem. Soc. 106*, 4926.

Riddle, V., & Lorenz, F. W. (1968) *J. Biol. Chem. 243*, 2718.

Sanderson, J. H., & Phillips, C. E. (1981) *An Atlas of Laboratory Animal Haematology*, Oxford University Press, Oxford.

Schimandle, C. M., & Vander Jagt, D. L. (1979) *Arch. Biochem. Biophys. 195*, 261.

Sellin, S., & Mannervik, B. (1983) *J. Biol. Chem. 258*, 8872.

Taft, R. W. (1957) in *Steric Effects in Organic Chemistry* (Newman, M. S., Ed.) Wiley, New York.

Vander Jagt, D. L., & Han, L.-P. B. (1973) *Biochemistry 12*, 5161.

Vander Jagt, D. L., Han, L.-P. B., & Lehman, C. H. (1972) *Biochemistry 11*, 3735.

Vander Jagt, D. L., Daub, E., Krohn, J. A., & Han, L.-P. B. (1975) *Biochemistry 14*, 3669.